Disentangling quantum matter with measurements

Daniel Ben-Zion, John McGreevy, and Tarun Grover
Department of Physics, University of California at San Diego, La Jolla, California 92093, USA

(Received 6 December 2019; revised manuscript received 12 February 2020; accepted 3 March 2020; published 18 March 2020)

Measurements destroy entanglement. Building on ideas used to study 'quantum disentangled liquids,' we explore the use of this effect to characterize states of matter. We focus on systems with multiple components, such as charge and spin in a Hubbard model or local moments and conduction electrons in a Kondo lattice model. In such systems, measurements of (a subset of) one of the components can leave behind a quantum state of the other that is easy to understand, for example in terms of scaling of entanglement entropy of subregions. We bound the outcome of this protocol, for any choice of measurement, in terms of more standard information-theoretic quantities. We apply this quantum disentangling protocol to several problems of physical interest, including gapless topological phases, heavy fermions, and scar states in the Hubbard model.

DOI: 10.1103/PhysRevB.101.115131

I. INTRODUCTION

Consider a quantum state of a two-component system, say, local moments interacting with electrons as in a Kondo lattice model or spin and charge degrees of freedom in a Hubbard model. How shall one characterize the quantum entanglement between the two components? One possible route is to integrate out one of the components and study the properties of the resulting reduced density matrix corresponding to the other component. Now one can characterize the entanglement between the two components via the von Neumann entropy of the resulting reduced density matrix. For example, if the two components were unentangled to begin with, then the reduced density matrix would be pure and therefore will have zero von Neumann entropy. At the other extreme, if the original wave function satisfies the eigenstate thermalization hypothesis (ETH), then the resulting density matrix will have a volume law von Neumann entropy [1–7]. A seemingly very different, and perhaps more feasible approach from an experimental standpoint, is to perform a *measurement* on only one of the components such that the state of that component is fully specified and study the resulting wave function. Basic principles of quantum mechanics dictate that the measurement renders the measured degrees of freedom as classical objects with definite values, and now the only quantum degrees of freedom belong to the unmeasured component. One measure of the entanglement between the two components is the *change* in the entanglement between different subsystems of the unmeasured component due to the measurement. For example, if the two components were unentangled to begin with, then the measurement leaves the reduced density matrix of the unmeasured component completely unchanged.

One application of such a partial-measurement-based protocol was discussed in Ref. [8], where a new state of matter, called 'quantum disentangled liquid' (QDL), was introduced. In a QDL state, measurement leads to a dramatic reduction in the bipartite entanglement of the unmeasured component ('disentangling'). Specifically, in such a phase, although the original wave function has a volume law bipartite entanglement, the unmeasured component only has area-law entanglement post measurement. It was argued that in contrast, in a conventional 'non-QDL' system, a similar protocol will instead lead to volume law entanglement for the unmeasured component post measurement. A physical picture [8] is that one component consists of 'heavy' particles, whose positions provide a disorder potential which can Anderson/many-body localize the 'light' particles. A context in which the physics of QDL is realized is the Hubbard model in $1+1$ dimensions [9,10], where the role of 'heavy' and 'light' particles is played by the spin and charge degrees of freedom, respectively. Strong numerical evidence was found that a band of QDL-like states survives the breaking of integrability [11]. These are examples of 'scar states'—states in the middle of the spectrum of a nonintegrable system that are not ergodic (in a many-body system, this means that they violate ETH).

In this paper we will show that the two seemingly different ways to characterizing entanglement introduced above—integrating out versus partial measurement—are intimately related. We will bound the outcome of the QDL protocol in terms of various *conditional information measures*—combinations of von Neumann entropies of subsystems, which can be interpreted as a quantum analog of conditioning on the subset of measured degrees of freedom. Specifically, we will show in Sec. I A that a specific kind of conditional entropy provides a lower bound on the expected entanglement of a state after a partial measurement. We also give (less-effective) upper and lower bounds on an alternate version of the QDL protocol in terms of conditional mutual information (CMI).

One practical advantage of the conditional information measures is that, in contrast to the measurement-based protocol, they are operator agnostic—they do not depend on a choice of which operator to measure. Relatedly, in an exact diagonalization study, implementation of conditional information measures do not involve averaging over any degrees of freedom, in contrast to measurement-based protocol where one needs to average over the outcome of a measurement, which can be time consuming.

 ©2020 American Physical Society

As just discussed, entanglement after partial measurement has so far been used as a tool to characterize scar states, or more generally, to address questions related to quantum thermalization in closed many-body systems. We will show that this set of ideas has much broader applications and is especially useful in characterizing entanglement in ground states of multicomponent systems. As an example, in Sec. IV we will characterize a 'gapless topological phase' in a model of spinful bosons where the charge degrees of freedom form a Luttinger liquid, while the spin degrees of freedom represent a symmetry protected topological (SPT) phase which is decoupled from the charge degrees of freedom at low energies. Specifically, we will show that measuring the charge degrees of freedom results in a gapped SPT wave function of spins, where the edge states in the entanglement spectrum are now much more apparent compared to those in the entanglement spectrum of the full gapless wave function. The post-measurement wave function can also be used to understand phase transitions in the spin sector between a SPT phase and a non-SPT phase.

As another application to ground state wave functions of correlated electrons, we will characterize phases relevant to Kondo lattice systems using conditional mutual information. In Sec. VI, we will show that in a heavy Fermi liquid, within a mean-field description, the entanglement of local moments conditioned on conduction electrons violates the area-law entanglement scaling in the manner of a Fermi liquid, thus exposing the underlying large Fermi surface which includes the local moments. We will also discuss the utility of conditional mutual information in diagnosing topological order in a fractionalized Fermi liquid, where at low energies local moments decouple from the conduction electrons and become topologically ordered.

We return in Sec. II to the notion of QDL in a Hubbard model discussed in Ref. [11] and study it from the perspective of conditional information measures. We will show that the 'scar states' where spin degrees of freedom effectively decouple from the charge degrees of freedom have a distinctive footprint in both conditional entropy and CMI, similar to the signature in the measurement-based diagnostic.

In Sec. III we observe that the entanglement negativity can also be used to distinguish QDL behavior from ergodicity. This is a measure of the bipartite entanglement in a mixed state which vanishes in separable states $\sum_c \rho_A^c \otimes \rho_B^c$—it is a measure of quantum entanglement and not classical correlations. A QDL state is precisely one where the entanglement of the light degrees of freedom alone is area law, whereas a general ergodic state has longer-range entanglement. We identify a precise situation where a sharp distinction can be made and verify the expected behavior in the Hubbard model. We note that the quantity called *SPT entanglement*, defined in Ref. [12] and shown there to label SPT states (at least for Abelian groups), is an example of a measurement-based protocol similar to the ones we study.

A. A bound on the QDL diagnostic

Following the discussion in Ref. [8], consider a measurement on the degrees of freedom belonging to only one component in a two-component system. A measurement effectively freezes the measured degrees of freedom to the outcome of the measurement. In the resulting wave function, the only quantum fluctuations correspond to the unmeasured component, and the probabilities associated with these quantum fluctuations can therefore be thought of as *conditional* probabilities—they are conditioned on the outcome of the measurement. This motivates us to seek a connection between the measurement based QDL diagnostic of Ref. [8] and *conditional entropy* (CE).

To build such a connection, we recall some general aspects of the QDL diagnostic. Consider a Hilbert space $\mathcal{H} = A \otimes B \otimes C$ with three parts. The QDL protocol takes as input a state ρ_{ABC} and a choice of operator X_C on C. We will assume that the outcomes of X_C provide a nondegenerate basis for C, so a measurement of X_C with outcome c completely specifies the state of C to be $|c\rangle$. The protocol is:

(1) Measure X_c and obtain outcome c with probability $p_c = \mathrm{tr}_{AB}\langle c|\rho_{ABC}|c\rangle$.

(2) In the resulting state ρ_{AB}^c find the von Neumann entropy of subsystem A, $S(\rho_A^c \equiv \mathrm{tr}_B \rho_{AB}^c)$.[1]

(3) Average over the distribution p_c to obtain the QDL diagnostic

$$S_{\mathrm{QDL}}(A|X_C) \equiv \sum_c p_c S\left(\rho_A^c\right).$$

A related quantity which depends on a state ρ_{ABC} but not a choice of operator is the *conditional entropy* of A conditioned on C[2]

$$S(A|C) \equiv S_\rho(AC) - S_\rho(C).$$

Classically, the conditional entropy is the Shannon entropy of the conditional probability distribution $p(a|c)$; quantum mechanically it is not the von Neumann entropy of any state and indeed can be negative. Its being negative is a sign that subsystems A and C are entangled. The conditional entropy has an operational meaning [13] in terms of the number of qubits from A needed for C to reconstruct their joint state ρ_{AC} given free local operations and classical communication; when it is negative it means that their entanglement can be used as a resource, for example to teleport quantum information from C to A.

We now show that the conditional entropy is a lower bound for the QDL diagnostic for any X_C:

$$S(A|C) \leqslant S_{\mathrm{QDL}}(A|X_C). \tag{1.1}$$

Proof. First, we note that the conditional entropy can be rewritten in terms of a *relative entropy*, $D(\rho||\sigma) \equiv \mathrm{tr}\rho\log\rho - \mathrm{tr}\rho\log\sigma$, as follows:

$$S(A|C) = A - D(\rho_{AC}\|u_A \otimes \rho_C) \tag{1.2}$$

[1]Since ρ_{AB}^c is a mixed state, this includes entropy of mixture, in addition to entropy of entanglement. With this in mind, we study instead a measure of mixed-state entanglement (the logarithmic negativity) in Sec. III.

[2]For a subsystem A and a density matrix ρ on a larger system we denote the von Neumann entropy $S_\rho(A) = S(\rho_A) = -\mathrm{tr}\rho_A\log\rho_A$, with $\rho_A \equiv \mathrm{tr}_{\bar{A}}\rho$. When there is no ambiguity about the density matrix in question, we will write $S(A)$.

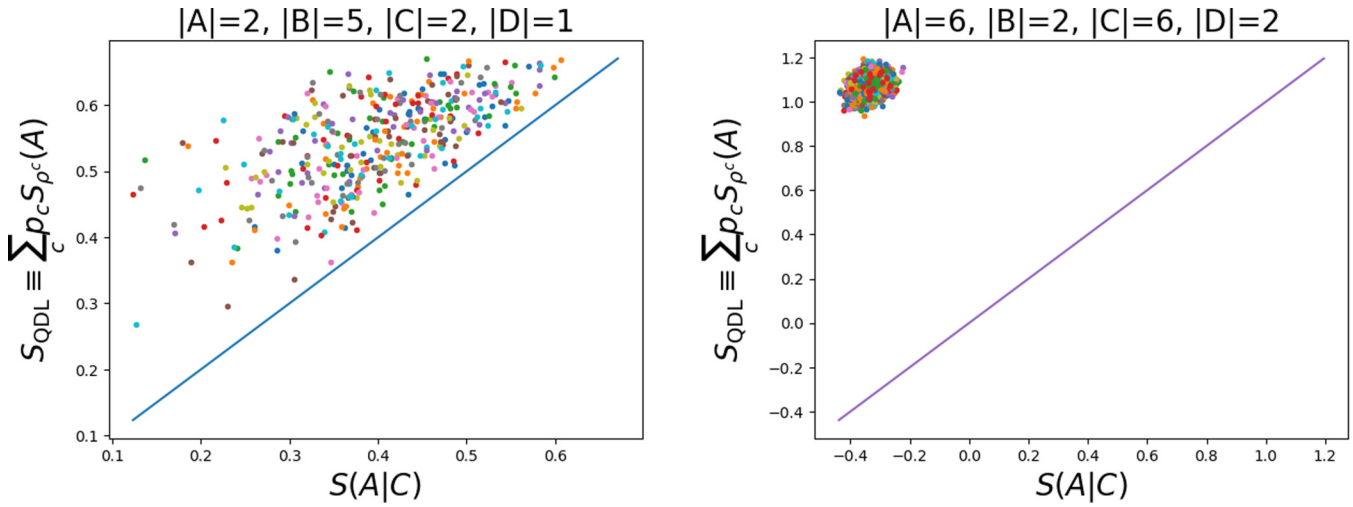

FIG. 1. Comparison of the conditional entropy $S(A|C)$ with the QDL quantity $S_{\rm QDL} \equiv \sum_c p_c S_{\rho^c}(A)$ for several Haar random states of $ABCD$, with $ABCD$ of the given dimensions. Left: For some values of subsystem sizes, the bound is seen to be fairly tight. Right: In other cases, as when $S(A|C)$ is negative, the bound is loose. Negative $S(A|C)$ is an indication that subsystems A and C are entangled more with each other than with the rest of the world.

where u_A is the uniform density matrix on $\mathcal{H}_A$, $u_A \equiv \mathbb{1}_A/\dim \mathcal{H}_A$, and we find it convenient to use $A \equiv \log \dim \mathcal{H}_A$ to denote the size of region A.

The rewriting (1.2) is useful because the relative entropy is monotonic under the action of any quantum channel $\mathcal{E}$

$$D(\rho||\sigma) \geqslant D(\mathcal{E}(\rho)||\mathcal{E}(\sigma)). \tag{1.3}$$

Consider in particular the diagonal-part channel on C in the basis of eigenstates $|c\rangle_C$ of $\mathcal{O}_C$, defined as:

$$\rho_{ABC} \mapsto \mathcal{E}(\rho_{ABC}) \equiv \sum_c \langle c|\rho_{ABC}|c\rangle \otimes |c\rangle\langle c| \equiv \sum_c p_c \rho^c_{AB} \otimes |c\rangle\langle c|. \tag{1.4}$$

This is the state that obtains if X_C is measured, but the outcome of the measurement is not known.

The key step is

$$S(A|C) \overset{(1.3)}{\leqslant} A - D(\mathcal{E}_C(\rho_{AC})||\mathcal{E}_C(u_A \otimes \rho_C)) \tag{1.5}$$

$$= \sum_c p_c S\left(\rho^c_A\right) = S_{\rm QDL}(A|X_C). \tag{1.6}$$

The right equality is shown in great detail in Appendix A. Therefore,

$$S(A|C) \leqslant S_{\rm QDL}(A|X_C),$$

a lower bound on the QDL quantity. ■

How tight is the bound we just proved? To learn something about this, in Fig. 1 we show the QDL diagnostic versus conditional entropy for a collection of Haar-random states, for various choices of partitions of some small Hilbert spaces. By Haar-random states we mean states of the form $U|\psi_0\rangle$ where $|\psi_0\rangle$ is some reference state (here, a product state) and U is a unitary sampled from the Haar measure.

As a side remark, we note the relevance of the notion of "quantum discord" [14,15] to this discussion. This quantity was introduced in attempts to distinguish between quantum and classical correlations in a given quantum state. Given a bipartite density matrix ρ_{AC} and a measurement X on C, the discord is defined to be

$$\begin{aligned}\text{discord}(\rho_{AC}, X) &\equiv S_A + S_C - S_{AC} - \chi(p_c, \rho^c) \\ &= -S(A|C) + S_{\rm QDL}(A|X_C),\end{aligned} \tag{1.7}$$

the difference between the QDL quantity and our lower bound for it. In the middle step, $\chi(p_c, \rho^c) \equiv S(\sum_c p_c \rho_c) - \sum_c p_c S(\rho_c)$ is the Holevo quantity, which will reappear below in Sec. V. The Holevo quantity provides a bound on the amount of classical information that can be sent by a quantum channel. (The discord of ρ itself is defined by extremizing over the choice of measurement on C.)

B. Distinguishing QDL and ergodic states with conditional entropy

The conditional entropy is capable of distinguishing between QDL and ergodic states. To do this, we further bipartition each subsystem into spatial regions, that is, divide the system into $ABCD$ where A, B are light and C, D are heavy. We assume the total system size is $L = A + B = C + D$.

For the purposes of this argument, to describe an ergodic state, we will use Page's rule [16]:

$$S_{\rm ergodic}(A) = \min(A, \bar{A})$$

where A denotes the system size, $\dim H_A \sim e^A$. Therefore when $A + C$ is less than half the system

$$S_{\rm ergodic}(A|C) = S(AC) - S(C) = (A + C) - C = A \tag{1.8}$$

has a volume law in the size of A.

To describe a QDL state, we will use the model QDL wave function on a system of two types of hardcore bosons from [8]:

$$\Psi_{\mathrm{QDL}}(N,n)=\psi(N)\prod_{j=1}^{L}\frac{1}{\sqrt{2}}\left(\delta_{n_j,0}+e^{\mathbf{i}\pi N_j}\delta_{n_j,1}\right). \tag{1.9}$$

$n_j=0,1$ are the light degrees of freedom and $N_j=0,1$ are the heavy degrees of freedom. $\psi(N)$ is an ergodic wave function. When necessary, we assume that it is $\psi(N)=\mathrm{sgn}(\{N_j\})2^{-L/2}$, independently random signs for each configuration of the heavy degrees of freedom.

First let us determine S_C. The reduced density matrix is

$$\begin{aligned}\rho_C(N_C,N_C')&=\sum_{n,N_D}\Psi_{\mathrm{QDL}}(N_C,N_D,n)\Psi^{\star}_{\mathrm{QDL}}(N_C',N_D,n) &(1.10)\\ &=\sum_{N_D}\psi(N_C,N_D)\psi^{\star}(N_C',N_D)\prod_{j\in C}\left(\frac{1+e^{\mathbf{i}\pi(N_j+N_j')}}{2}\right)\\ &=\delta_{N_C,N_C'}\sum_{N_D}|\psi(N_C,N_D)|^2. &(1.11)\end{aligned}$$

If we use the random-sign form of the wave function, this is a diagonal density matrix all of whose eigenvalues are equal (to 2^{-C}), so the entropy is maximal. To estimate the entropy more generally we can compute the purity $S_2(\rho_C)\equiv -\log\mathrm{tr}\rho_C^2\leqslant S(\rho_C)$.

$$\begin{aligned}\mathrm{tr}\rho_C^2&=\sum_{N_C,N_C'}\rho(N_C,N_C')\rho(N_C',N_C)\\ &=\sum_{N_C}\left(\sum_{N_D}|\psi(N_C,N_D)|^2\right)^2=2^{-C},\end{aligned}$$

and therefore $S_2(\rho_C)=C\log 2$ is volume law in the size of C. Since $S_2\leqslant S_{vN}$, this implies that the von Neumann entropy is also volume law.

In the case where $A=C$, the calculation of S_{AC} is done in Ref. [8]. We give the more general calculation for $A<C$ because it will be useful below:

$$\begin{aligned}&\rho_{AC}(N_C,n_A;N_C',n_A')\\ &\quad=\sum_{N_D,n_B}\Psi_{\mathrm{QDL}}(N_C,N_D,n_A,n_B)\Psi_{\mathrm{QDL}}(N_C',N_D,n_A',n_B) &(1.12)\\ &\quad=f(N_C,n_A)f(N_C',n_A')\prod_{j\in C\setminus A}\left(\frac{1+e^{\mathbf{i}\pi(N_j+N_j')}}{2}\right)\\ &\qquad\times\sum_{N_D}\psi(N_C,N_D)\psi^{\star}(N_C',N_D) &(1.13)\end{aligned}$$

where, as in Ref. [8],

$$f(N,n)\equiv\prod_{j\in A}\frac{1}{\sqrt{2}}\left(\delta_{n_j,0}+e^{\mathbf{i}\pi N_A}\delta_{n_j,1}\right).$$

Then

$$\begin{aligned}\mathrm{tr}\rho_{AC}^2&=\sum_{N_C,N_C'}\underbrace{\sum_{n_A,n_A'}f(N_C,n_A)^2f(N_C',n_A')^2}_{=1}\prod_{j\in C\setminus A}\delta_{N_j,N_j'} &(1.14)\\ &\quad\times\sum_{N_D}\psi(N_C,N_D)\psi^{\star}(N_C',N_D)\sum_{N_D'}\psi(N_C',N_D')\psi^{\star}(N_C,N_D') &(1.15)\\ &\simeq\sum_{N_C=N_C'}\sum_{N_D,N_D'}2^{-2L}+\sum_{N_D=N_D'}\sum_{N_A,N_A'}\sum_{N_{C\setminus A}}2^{-2L}-\sum_{N_D=N_D'=N_C=N_C'}2^{-2L} &(1.16)\\ &=2^{C+2D-2L}+2^{D+2A+(C-A)-2L}-2^{C+D-2L} &(1.17)\\ &=2^{-C}+2^{A-L}-2^{-L}. &(1.18)\end{aligned}$$

Therefore in this case

$$S(AC)=-\log\mathrm{tr}\rho_{AC}^2=-\log(2^{-C}+2^{-D-C+A}-2^{-L}).$$

In the special case $A=C$, this is $S(AC)=-\log(2^{-C}+2^{-D}-2^{-L})$ in agreement with Ref. [8].

Therefore, in a QDL state, we expect

$$\begin{aligned}S(A|C)&=S(AC)-S(C)\\ &=-\log(2^{-C}+2^{-D-C+A}-2^{-L})-C\log 2.\end{aligned}$$

Setting $A=C=l$, for $l\ll L$ this behaves as

$$S(A|C)\overset{l\ll L}{\simeq}-2^{-L}l+\mathcal{O}(2^{-2L}l^2)\quad(A=C=l), \tag{1.19}$$

a *negative* volume law with a coefficient which vanishes exponentially with system size (Fig. 2, left).

If instead $A=l$ but we hold fixed $C=L/2$, then

$$S(A|C)\overset{l\ll L}{\simeq}-2^{-L/2}l+\mathcal{O}(2^{-L/2}l^2)\quad(A=l,C=L/2), \tag{1.20}$$

the (negative) volume-law coefficient still vanishes exponentially with system size but not as fast (Fig. 2, right). We will

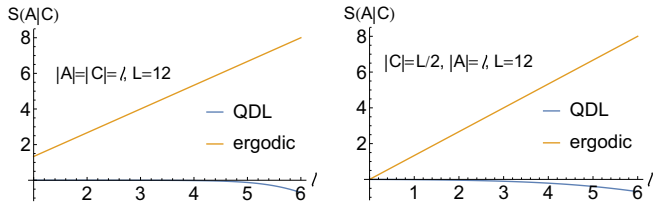

FIG. 2. Expectations for conditional entropy in a QDL state (blue) and an ergodic state (orange), based on (1.19) and (1.20). Left: when regions A and C are the same size, l. Right: when $|C|$ is fixed at $L/2$ and $|A| = l$.

compare this expectation with the behavior in scar states of the Hubbard model below in Sec. II.

C. Mutual information QDL diagnostic

An alternate protocol replaces the von Neumann entropy with the mutual information between A and B. That is, replace the latter two steps of the protocol by

(1) In the resulting state ρ^c_{AB} find the mutual information between A and B: $I_{\rho^c_{AB}}(A:B)$.

(2) Average over the distribution p_c to obtain an alternate QDL diagnostic

$$\overline{I_{X_C}(A:B|C)} \equiv \sum_c p_c I_{\rho^c_{AB}}(A:B).$$

When ABC is the full system, and measuring X_C completely fixes the state of C, then ρ^c_{AB} is a pure state. To see this explicitly, write the initial state $|\psi_{ABC}\rangle$ in the basis of eigenstates of the operator X_C:

$$|\psi_{ABC}\rangle = \sum_c |\psi_{AB}(c)\rangle \otimes |c\rangle.$$

Then by the axioms of quantum mechanics, when we measure X_C and get the outcome c, the resulting state (up to normalization) is

$$|\psi_{ABC}\rangle \overset{\text{measure } X_C, \text{ get } c}{\longrightarrow} |\psi_{AB}(c)\rangle \otimes |c\rangle,$$

a product state between AB and C, $\rho_{AB}|c = |\psi_{AB}(c)\rangle\langle\psi_{AB}(c)|$. In such a state the von Neumann entropy of AB vanishes, $S(\rho^c_{AB}) = 0$, and hence

$$I_{\rho^c_{AB}}(A:B) = S(\rho^c_A) + S(\rho^c_B) - S(\rho^c_{AB}) = 2S(\rho^c_A). \quad (1.21)$$

Averaging (1.21) over the distribution of outcomes p_c says that under these conditions, the mutual information version of the QDL diagnostic is twice the original QDL diagnostic:

$$\overline{I_{X_C}(A:B|C)} = 2\overline{S_{X_C}(A)} \quad \text{if } ABC \text{ is pure.}$$

A related quantity which depends on a state ρ_{ABC} but not a choice of operator is the conditional mutual information

$$\begin{aligned} I(A:B|C) &\equiv S_{AC} + S_{BC} - S_{ACB} - S_C \\ &= I(A:BC) - I(A:C) \quad (1.22) \\ &= D(\rho_{ACB}||\rho_A \otimes \rho_{BC}) - D(\rho_{AC}||\rho_A \otimes \rho_C) \quad (1.23) \end{aligned}$$

where $D(\rho||\sigma) \equiv \mathrm{tr}\rho\log\rho - \mathrm{tr}\rho\log\sigma \geqslant 0$ is the relative entropy. In Sec. V B we will bound the alternate QDL diagnostic in terms of the conditional mutual information.

II. CONDITIONAL ENTROPY AND QDL PHYSICS IN THE HUBBARD MODEL

To establish the utility of the diagnostics introduced in Sec. I, we compute the conditional entropy and conditional mutual information in the same model studied in Ref. [11]. We perform exact diagonalization of the one-dimensional Hubbard model with a repulsive nearest neighbor interaction added to break integrability

$$\mathbf{H} = -t\sum_{i\sigma} c^\dagger_{i\sigma}c_{i+1\sigma} + U\sum_i n_{i\uparrow}n_{i\downarrow} + V\sum_i n_i n_{i+1} \quad (2.1)$$

where $n_{i\sigma} \equiv c^\dagger_{i\sigma}c_{i\sigma}$ and $n_i \equiv \sum_\sigma n_{i\sigma}$.

Given an eigenstate of $\mathbf{H}$, we compute the conditional entropy $S(A|C)$ for a subset of the charges (the light degrees of freedom), conditioned on a subset of the spins (the heavy degrees of freedom). We partition the system as in Fig. 3, so that subsystem A is all the charge degrees of freedom on

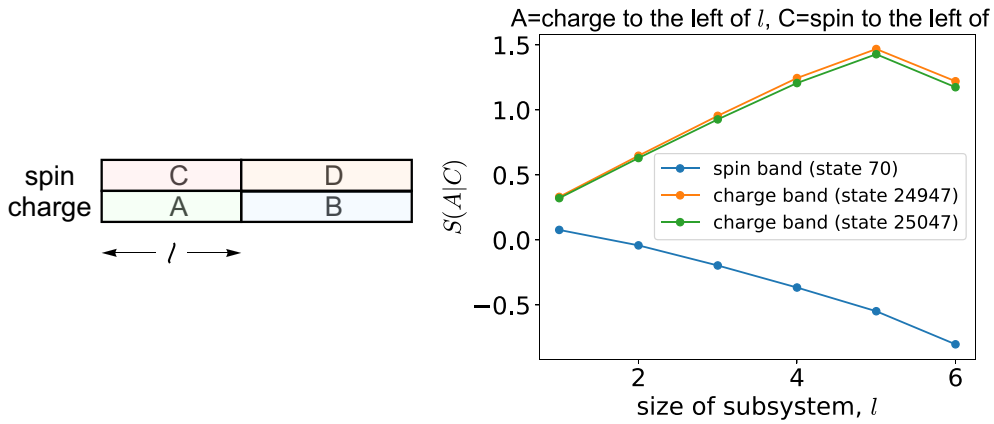

FIG. 3. Left: Partition of the Hubbard model degrees of freedom. A (C) is chosen to be the charge (spin) degrees of freedom on sites 1 through l. Right: Conditional entropy in a one-dimensional Hubbard model as a function of the location of the bipartioning cut at couplings $U = 4$, $V = 3/4$. The chain is periodic and has $L = 12$ sites, the particle number is at half filling, and the magnetization is zero. We show the result for two charge band states and one spin band state, which can be compared, respectively, with (1.8) and (1.19).

sites 1 through l, B is the remainder of the charges, C is all the spins on sites 1 through l, and D is the remainder of the spins.

In Fig. 3 we show the result for the conditional entropy $S(A|C) = S(AC) - S(C)$ in several eigenstates. Our results confirm those of Ref. [11], and the striking difference in behavior between ergodic and QDL states illustrates the utility of conditional entropy as a proxy for observing QDL behavior. The behavior sharply distinguishes QDL and ergodic behavior, in agreement with our expectations from Sec. I B. In particular, in the case of a QDL state, the slope of $S(A|C)$ as a function of the size of A is indeed negative. A more quantitative comparison is obstructed by the small system size. The discussion of the conditional mutual information can be found in Appendix B.

III. QDL AND NEGATIVITY

For mixed states, the von Neumann entropy is not a good measure of entanglement, since it includes also classical uncertainty. A computable measure of entanglement for mixed states is the logarithmic negativity [17,18], defined as $E_N(\rho) \equiv -\log|\rho^{T_A}| = -\log(\sum_a |\lambda_a|)$, where λ_a are the eigenvalues of ρ^{T_A}, the partially transposed density matrix, $\rho^{T_A}_{ab,a'b'} \equiv \rho_{a'b,ab'}$.

In a QDL state, the reduced density matrix for the 'light' particles is essentially separable, because $\rho_A = \sum_c p_c \rho_A(c)$ and each $\rho_A(c)$ is area law due to QDL-ness. Therefore the negativity is area law for this mixed state. This result holds irrespective of the size of the Hilbert space of the 'heavy' particles, and as we now show, leads to a new diagnostic for the QDL states when the Hilbert space of heavy particles is smaller than half the total Hilbert space.

The area law of negativity is not necessarily a very striking characterization because negativity is area law even for a Gibbs state [19]. Such a thermal state is obtained by tracing out more than half the degrees of freedom in a purely ergodic wave function. In contrast, for an ergodic wave function, integrating out *less than half* the degrees of freedom leads to a *volume law negativity* [20,21]. The intuition is that nothing dramatic happens if one integrates out a very small region, so negativity will continue to be volume law until the subsystem looks thermal. This intuition is verified numerically in ergodic spin chains [20] and proved analytically for Haar random states [21].

Therefore, when the Hilbert space of heavy particles is smaller than half the total Hilbert space, then the area law of negativity is another way to quantify QDL behavior. This expectation is verified in Fig. 4.

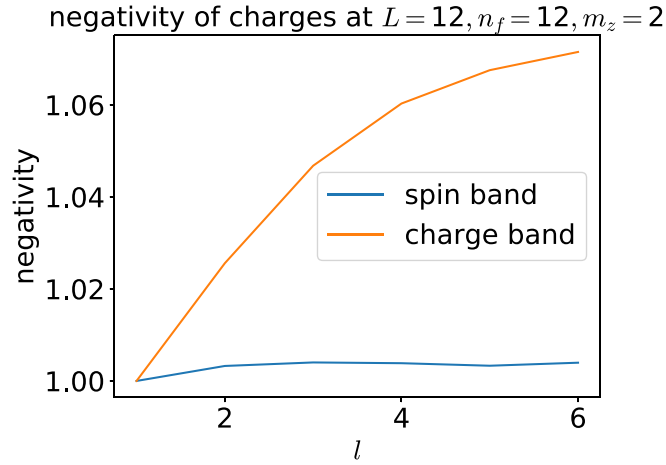

FIG. 4. The logarithmic negativity for a spin-band state and a charge-band state of the deformed Hubbard model. Here the magnetization is chosen to be $m_z = 2$, at half filling, so that the spin (heavy) Hilbert space is smaller than the charge (light) Hilbert space.

IV. DETECTING SPT PHYSICS IN A GAPLESS SYSTEM VIA PARTIAL MEASUREMENT

We now turn to applications of QDL-based protocols to questions about interesting ground states of condensed matter. We consider a model of spin 1 hardcore bosons governed by the Hamiltonian

$$\mathbf{H} = -t \sum_{i\sigma} b^\dagger_{i\sigma} b_{i+i\sigma} + \text{H.c.} + J \sum_i \vec{S}_i \cdot \vec{S}_{i+1} + D \sum \left(S^z_i\right)^2. \tag{4.1}$$

The hopping amplitude t determines an overall energy scale and we set it equal to 1. This model was originally considered in Ref. [22] as a strong coupling limit of a particular two leg fermionic ladder; the spinful hardcore boson represents two fermions bound into a triplet state across a rung of the ladder.

In addition to a trivial paramagnet phase, a spin-1 chain also possesses a nontrivial SPT phase known as the Haldane phase [23–25]. In Ref. [22], the model in (4.1) was argued to exhibit spin-charge separation in the sense that the ground state wave function factorizes into a charge wave function times a spin wave function on the squeezed lattice (the lattice obtained by deleting the unoccupied sites). As a result of this spin-charge separation, it was argued that the spin degrees of freedom can form an SPT phase, despite the presence of the gapless charge degrees of freedom.

Here we apply the QDL protocol to freeze the charge degrees of freedom and study the entanglement properties of spins in the resulting wave function. For a conventional spin wave function, one signature of an SPT phase is a degeneracy in the entanglement spectrum due to the edge modes [26]. We therefore propose to use the entanglement spectrum of the post-projection wave function to access the topological properties of the state.

The ground state of (4.1) was obtained for both open and periodic boundary conditions using DMRG, with bond dimensions up to $\chi = 3000$. Figure 5 shows the post-projection entanglement spectra in the topological phase ($J \gg D$). It is very easy to see the systematic double degeneracy throughout the entire entanglement spectrum. As we increase D and go over to the trivial phase, the degeneracy disappears as expected.

In addition to the entanglement spectrum, we can look at the entanglement entropy of the post-projection wave function. In particular, we study $S_{\text{QDL}}(c, A) \equiv \sum_c p_c S(\rho^c_A)$ where p_c is the probability of finding a particular configuration c of the (measured) charge degrees of freedom, and ρ^c_A denotes the density matrix corresponding to the (unmeasured) spin degrees of in a subregion A.

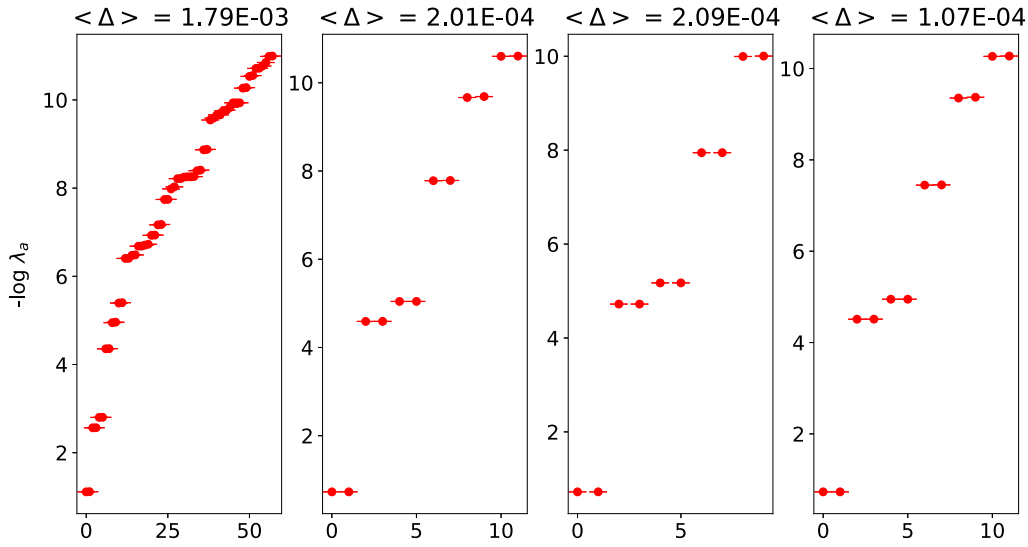

FIG. 5. Leftmost: Entanglement spectrum across the center bond of the full wave function. Right plots: Entanglement spectrum across the center bond for the projected wave function $|\Psi_s\rangle$ for three randomly chosen hole configurations. The system size is $L = 96$, with couplings $J = 0.1$ and $D = 0.01$. Also shown is the mean spacing between pair levels in the entanglement spectrum $\langle\Delta\rangle$.

We studied (4.1) at system size $L = 64$ with periodic boundary conditions. It is somewhat impractical (and in general impossible) to average over all charge configurations, so we calculated $S_{\rm QDL}$ via Monte Carlo sampling with the distribution p_c. The results in the topological phase, in the trivial phase, and directly at the critical point are shown in Fig. 6. In all cases, the entanglement entropy as a function of subsystem size for the full wave function (with no projection) has the form

$$S(l) \sim \frac{c}{3}\log\left(\frac{L}{\pi}\sin\left(\frac{\pi l}{L}\right)\right) + b \tag{4.2}$$

with $c = 1$ away from the critical point and $c = 2$ at the critical point. Away from the critical point, the spins are essentially in a gapped phase which mixes very weakly with the gapless charge degrees of freedom, so we see $c = 1$ worth of gapless charge.

Applying the QDL projection freezes the charge degrees of freedom; the entanglement entropy of the post-projection wave function collapses into an area law behavior characteristic of a gapped phase in one dimension. At the critical point, the post-projection wave function retains the entanglement entropy of a critical wave function (4.2) with precisely $c = 1$, in line with the fact that the spins are in a $c = 1$ state at the critical point.

As far as we are aware, performing partial projections and studying properties of the 'leftover' wave function has not been generally explored in the context of ground state wave functions.[3] The distinction between an SPT and a trivial phase is typically predicated on the existence of a finite energy gap in both phases [27]. However there appear to be examples where features usually associated with SPT phases persist in the presence of gapless modes, including the model studied in this section as well as the models described in Ref. [28]. Quantum disentangling is likely to provide a useful method for studying such systems.

V. MORE BOUNDS ON THE OUTCOME OF THE QDL PROTOCOL

A. An upper bound on the QDL quantity

Here we give an upper bound on the QDL quantity in terms of information theoretic objects. The Holevo bound is a lower bound on the Holevo quantity

$$\chi\left(\{p_c, \rho_A^c\}\right) \equiv S\left(\sum_c p_c\rho_A^c\right) - \sum_c p_c S\left(\rho_A^c\right) \tag{5.1}$$

(the entropy of the average density matrix minus the average of the entropies) in terms of the mutual information between the distribution p_c (call it X) and that of any measurement Y that can be done on A:

$$0 \leqslant H(X:Y) \leqslant \chi.$$

We use the letter H to emphasize that $H(X:Y)$ is the mutual information between two classical distributions. By subtraction, this implies that the QDL quantity is bounded above:

$$\sum_c p_c S\left(\rho_A^c\right) = S\left(\sum_c p_c\rho_A^c\right) - \chi \leqslant S\left(\sum_c p_c\rho_A^c\right) - H(X:Y).$$

The bound gets stronger the bigger is $H(X:Y)$.

The average density matrix is just[4]

$$\sum_c p_c\rho_A^c = \mathrm{tr}_{BC}\rho_{ABC} = \rho_A.$$

[3] As we noted above, an interesting exception is Ref. [12], which however does not study gapless states.

[4] To check this, we can purify ρ_{ABC} by a state $|\psi\rangle_{ABCD}$. Then

$$(\rho_A)_{aa'} = \sum_c\sum_{bd}\psi^c_{abd}\psi^{\star c}_{a'bd} = \sum_c p_c(\rho_A^c)_{aa'}.$$

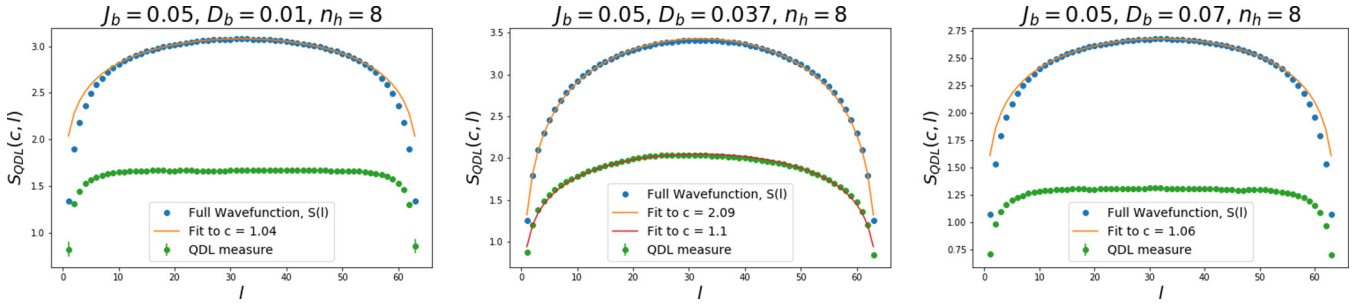

FIG. 6. QDL Measure $S_{\mathrm{QDL}}(c, l)$ across the phase diagram. (Left) Topological phase: entanglement entropy of post-projection spin wave function collapses to an area law. (Middle) Critical point: entanglement entropy of post-projection spin wave function shows critical behavior with central charge $c = 1$. (Right) Trivial phase: entanglement entropy of post-projection spin wave function collapses to an area law.

So the first term on the RHS is $S(\sum_c p_c \rho_A^c) = S_A$. Therefore

$$S_{\mathrm{QDL}} \leqslant S_A - H(X:Y). \tag{5.2}$$

So, at the weakest, we have $S_{\mathrm{QDL}} \leqslant S_A$ (which follows from concavity of the von Neumann entropy).

To improve upon this estimate, we must ask: As we vary the choice of measurement Y, how large can $H(X:Y)$ get? The largest it can be is called the *accessible information*

$$\mathcal{I} \equiv \max_Y H(X:Y). \tag{5.3}$$

We note that

$$H(X:Y) \leqslant I(A:C). \tag{5.4}$$

This follows from (1.3) because the distribution $p_{xy}|x\rangle \otimes |y\rangle$ is the state that results from measuring the operators X, Y on $A \otimes C$ and not looking at the answer. A lower bound on the accessible information just in terms of $\rho_A = \sum_c p_c \rho_A^c$ is given in Ref. [29], but is not useful for our purposes, because the bound (the "subentropy" of ρ_A) is itself a bounded quantity, independent of the size of $\mathcal{H}_A$. In Haar random states, numerical experiments (Fig. 7) show that the inequality (5.4) is far from saturated on average.

B. QDL mutual information and CMI

Denoting the QDL mutual information

$$\overline{I_{X_C}(A:B|C)} \equiv \sum_c p_c I_{\rho_{AB}^c}(A:B) \equiv I_{\mathrm{QDL}},$$

we will show that it can be bounded above and below in terms of the conditional mutual information:

$$I_\rho(A:B|C) - (I_\rho(AB:C) - I_{\mathcal{E}\rho}(AB:C)) \leqslant I_{\mathrm{QDL}} \leqslant I_\rho(A:B|C) + (I_\rho(A:C) - I_{\mathcal{E}\rho}(A:C)). \tag{5.5}$$

Here $\mathcal{E}$ is the quantum channel (1.4) associated with the measurement X_C. The quantity appearing in the error terms $I_{\mathcal{E}\rho}(A:C) = \chi(\rho_A^c, p_c)$ is again the Holevo quantity. Moreover, in both the lower and upper bound, $I_\rho(A:C) - I_{\mathcal{E}\rho}(A:C)$ is again the quantum discord.

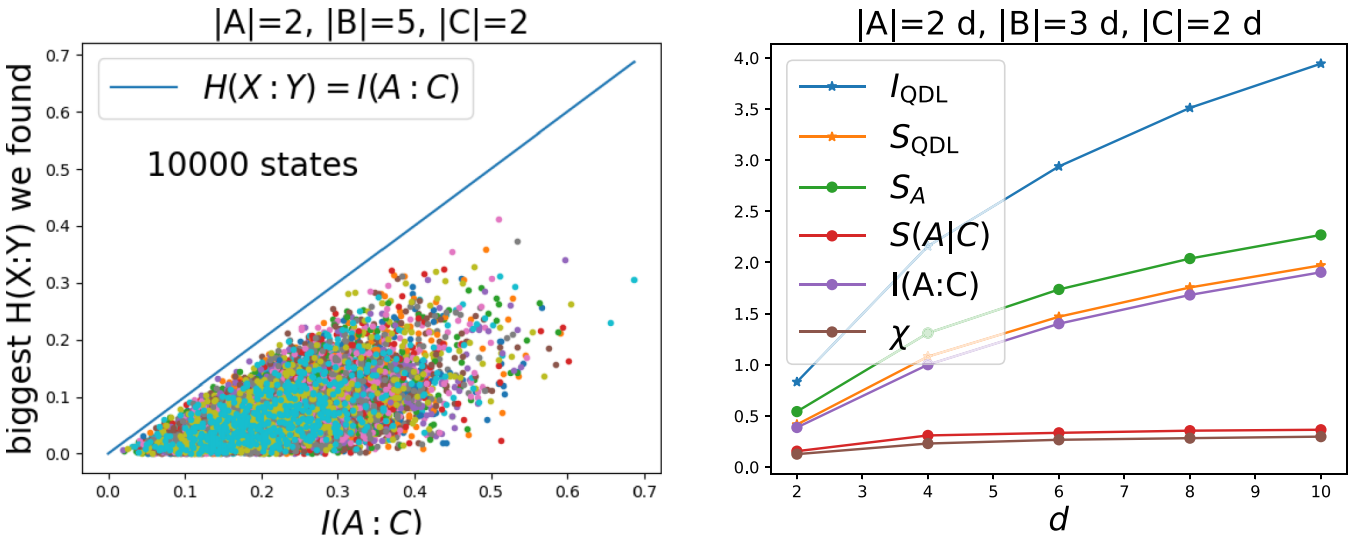

FIG. 7. Left: Lower bounds on the accessible information between A and C versus the mutual information $I(A:C)$ in many Haar-random states on ABC of the indicated dimensions. Each dot represents a state of ABC; the vertical position is the largest value of $H(X:Y)$, optimizing over measurements Y on A. We see that there are random states for which the Holevo bound is tight, but on average it is far from being saturated. Right: various quantities considered in this paper, averaged over 100 Haar-random states on ABC, as a function of Hilbert space size, with ratios of dimensions of A, B, C held fixed.

To see the upper bound on I_{QDL}, use (1.3) in the first term of

$$I_\rho(A:B|C) = D(\rho_{ABC}||\rho_A\otimes\rho_{BC}) - D(\rho_{AC}|\rho_A\otimes\rho_C) \tag{5.6}$$

$$\geqslant D(\mathcal{E}\rho_{ABC}||\mathcal{E}(\rho_A\otimes\rho_{BC})) - D(\rho_{AC}|\rho_A\otimes\rho_C) \tag{5.7}$$

$$= S_{\mathcal{E}\rho}(A) + S_{\mathcal{E}\rho}(BC) - S_{\mathcal{E}\rho}(ABC) - I_\rho(A:C). \tag{5.8}$$

In terms of the spectral decomposition of $\rho^c_{AB} = \sum_i \lambda_i^{(c)}|\lambda_i^{(c)}\rangle\langle\lambda_i^{(c)}|$, in the state (1.4) we have

$$S_{\mathcal{E}(\rho)}(ABC) = \sum_c p_c \sum_i \lambda_i^{(c)} \log p_c\lambda_i^{(c)} = H(p) + \sum_c p_c S\left(\rho^c_{AB}\right)$$

and similarly for $S_{\mathcal{E}(\rho)}(BC)$. In contrast, $S_{\mathcal{E}\rho}(A) = S(\sum_c p_c\rho^c_A)$. Use (1.3) in the first term of

$$I_\rho(A:B|C) \geqslant S\left(\sum_c p_c\rho^c_A\right) + H(p) + \sum_c p_c S\left(\rho^c_B\right) - \left(H(p) + \sum_c p_c S\left(\rho^c_{AB}\right)\right) - I_\rho(A:C) \tag{5.9}$$

$$= \sum_c p_c\left(S\left(\rho^c_B\right) + S\left(\rho^c_A\right) - S\left(\rho^c_{AB}\right)\right) - \sum_c p_c S\left(\rho^c_A\right) + S\left(\sum_c p_c\rho^c_A\right) - I_\rho(A:C) \tag{5.10}$$

$$= \sum_c p_c I_{\rho^c_{AB}}(A:B) + S\left(\sum_c p_c\rho^c_A\right) - \sum_c p_c S\left(\rho^c_A\right) - I_\rho(A:C) \tag{5.11}$$

$$= \overline{I_{\mathcal{O}_c}(A|C)} + \chi\left(\{p_c, \rho^c_A\}\right) - I_\rho(A:C) \tag{5.12}$$

$$= \overline{I_{\mathcal{O}_c}(A|C)} + I_{\mathcal{E}\rho}(A:C) - I_\rho(A:C). \tag{5.13}$$

(Indicated in blue are terms which are added and subtracted.)

In the other direction, we can bound $I(A:B|C)$ from above in terms of the QDL mutual information:

$$I_\rho(A:B|C) = S_\rho(A|C) + S_\rho(B|C) - S_\rho(AB|C) \tag{5.14}$$

$$= -D(\rho_{AC}||\mathbb{1}_A\otimes\rho_C) - D(\rho_{BC}||\mathbb{1}_B\otimes\rho_C) - S_\rho(AB|C) \tag{5.15}$$

$$\overset{(1.3)}{\leqslant} -D(\mathcal{E}\rho_{AC}||\mathcal{E}\mathbb{1}_A\otimes\rho_C) - D(\mathcal{E}\rho_{BC}||\mathcal{E}\mathbb{1}_A\otimes\rho_C) - S_\rho(AB|C) \tag{5.16}$$

$$= S_{\mathcal{E}\rho}(AC) - S_{\mathcal{E}\rho}(C) + S_{\mathcal{E}\rho}(BC) - S_{\mathcal{E}\rho}(C) - S_\rho(AB|C) \tag{5.17}$$

$$= \sum_c p_c(S_{\rho^c}(A) + S_{\rho^c}(B)) - S_\rho(ABC) + S_\rho(C) \tag{5.18}$$

$$= \sum_c p_c I_{\rho^c}(A:B) + \sum_c p_c S_{\rho^c}(AB) + S_\rho(C) - S_\rho(ABC) \tag{5.19}$$

$$= I_{\mathrm{QDL}} + \sum_c p_c S_{\rho^c}(AB) + S_\rho(C) - S_\rho(ABC) \tag{5.20}$$

$$= I_{\mathrm{QDL}} + \sum_c p_c S_{\rho^c}(AB) - S_\rho(AB) + S_\rho(AB) + S_\rho(C) - S_\rho(ABC) \tag{5.21}$$

$$= I_{\mathrm{QDL}} - \chi\left(p_c, \rho^c_{AB}\right) + I_\rho(AB:C). \tag{5.22}$$

Note that

$$S_{\mathcal{E}\rho}(A|C) = \sum_c p_c S_{\rho^c}(A) + H(X) - H(X) = \sum_c p_c S_{\rho^c}(A).$$

We have not yet found an example where the error terms in the bound (5.5) do not scale with system size. Numerical experiments (Fig. 8) on random states show that while neither directly bounds the other, the IQDL quantity and the CMI exhibit the same scaling behavior.

VI. DISENTANGLING HEAVY FERMI LIQUIDS

We now turn to the applications to heavy-fermion physics. An elementary model for heavy fermion materials is the Kondo lattice model (KLM). The KLM consists of a lattice of localized moments $\vec{S}$ coupled to a sea of conduction electrons by spin exchange.

$$\mathbf{H}_K = \sum_k \epsilon(k) c^\dagger_k c_k + J_K \sum_i \vec{S}_i\cdot\vec{s}_i + J_H \sum_{\langle ij\rangle} \vec{S}_i\cdot\vec{S}_j \tag{6.1}$$

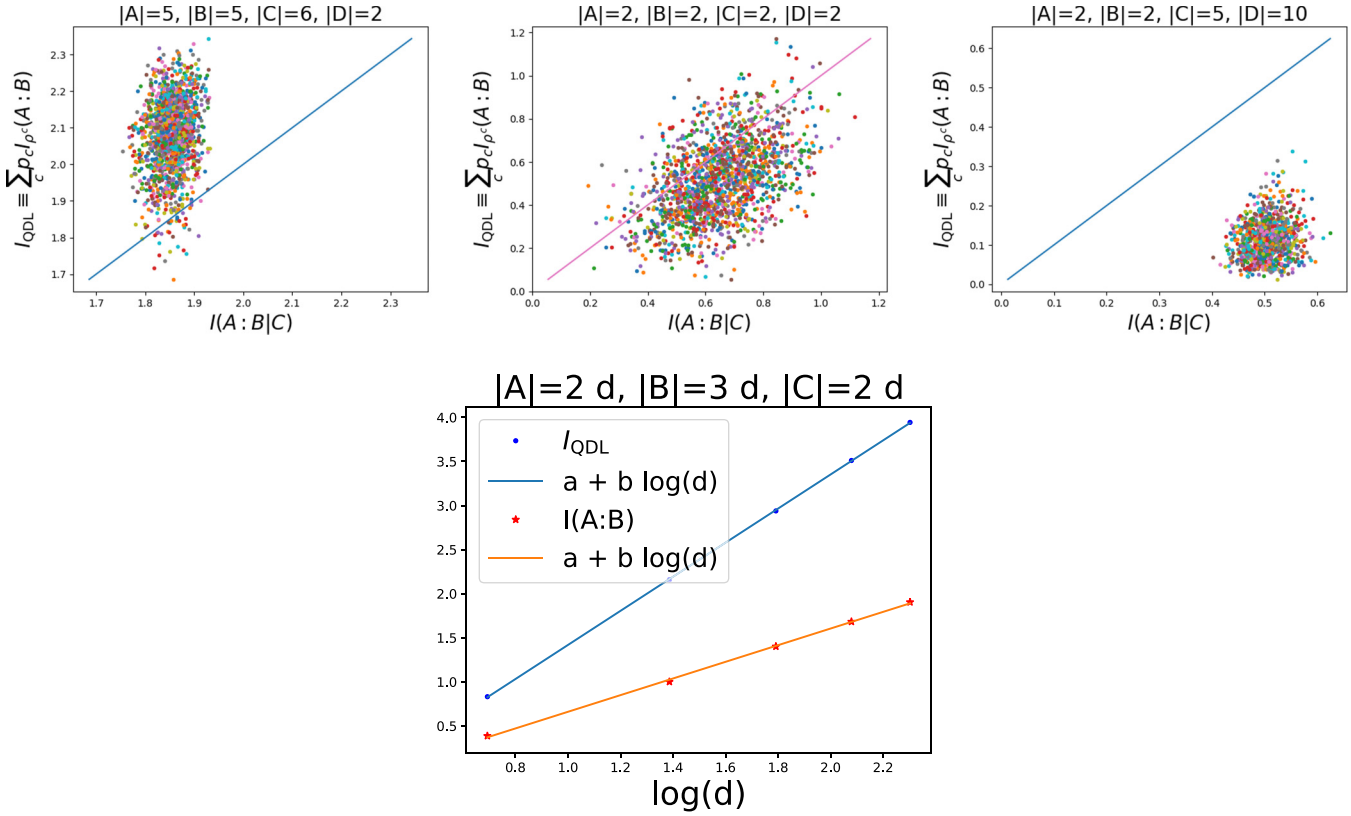

FIG. 8. Top: the I_{QDL} quantity versus $I(A:B|C)$ for many pure Haar-random states of $ABCD$, with $ABCD$ of the given dimensions. Bottom: a fit to the average behavior of both the I_{QDL} quantity and the CMI in Haar-random states as a function of the overall Hilbert space size d, holding fixed the ratios of dimensions of ABC ($|D| = 1$ here). Both exhibit a volume law in system size $\propto \log d$.

where $\vec{s} = \frac{1}{2} c_\alpha^\dagger \vec{\sigma}_{\alpha\beta} c_\beta$ is the electron spin. We have also included the possibility of antiferromagnetic exchange interactions between the local spins. This model has been extensively studied and exhibits several phases. The phase diagram is determined by a competition between an RKKY effect which favors a magnetically ordered state and the Kondo interaction. In addition to the heavy Fermi liquid (HFL) phase which has a large Fermi surface (FS), there is the possibility of an alternative paramagnetic state where the spins decouple from the conduction electrons and enter a spin-liquid state [30]. Such an 'FL* phase' is characterized by a fractionalized spin liquid coexisting with a small FS of conduction electrons.

One important distinction between the HFL phase and the FL* phase is that in the former, the conduction electrons and the local moments are entangled at long distances, while in the latter, they are not. One way to characterize this entanglement is to consider the mutual information between these two degrees of freedom in a given spatial region, as discussed in Refs. [31,32]. Within this scheme, one considers local moments f_A and conduction electrons c_A in a given subregion A and considers $S(f_A) + S(c_A) - S(f_A \cup c_A)$. One potential drawback of this quantity is that both $S(f_A)$ and $S(c_A)$ are sensitive to short distance entanglement between local moments and conduction electrons in region A and will generically be volume law. This short distance volume law entanglement is not canceled out by the subtracted term $S(f_A \cup c_A)$ which satisfies an area law up to multiplicative logarithmic corrections. Here we instead explore QDL inspired ideas to study the nature of entanglement between the spins and the conduction electrons. Compared to a mutual-information-based protocol, we will find that a QDL based protocol can be devised which is sensitive only to long distance entanglement.

In a system with a FS, the entanglement entropy of a region of linear size l will behave as $S(l) \sim l^{d-1} \log l$, a violation of the area law [33,34]. Consider measuring the positions of all conduction electrons in the ground state of the KLM. In an HFL state, the local moments participate in the Fermi surface, and we expect that the resulting wave function will continue to have the properties of a state with a Fermi surface, namely, $S(l) \sim l^{d-1} \log l$. In contrast, in the FL* state where the local moments form a gapped spin liquid, one expects that the resulting wave function satisfies $S(l) \sim l^{d-1} - \gamma$ where γ is the topological entanglement entropy corresponding to the topological order of the local moments. This is analogous to our discussion of gapless SPT state in Sec. IV, where the charge degrees of freedom form a Luttinger liquid, while the spin degrees of freedom form an SPT state.

Motivated by the discussion in Sec. V, we consider the conditional mutual information between two nonoverlapping sets of local moments A and B, conditioned on the state of all the conduction electrons C.

$$\begin{aligned} I(A:B|C) &= S_{AC} + S_{BC} - S_{ABC} - S_C \\ &= S_A + S_B - S_{AB} = I(A:B), \end{aligned} \tag{6.2}$$

where the last relation follows because ABC is the full system. We consider the system on a torus of dimensions $L_x \times L_y$ and

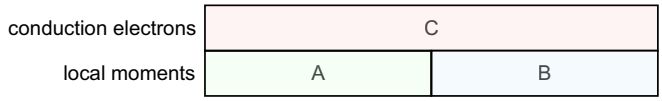

FIG. 9. Subsystems involved in the conditional mutual information which expose the Fermi surface behavior of the local moments.

cut the system at fixed x into two cylinders A and B. Due to the local Kondo hybridization, the entanglement entropy of local moments will be dominated by a volume law. Schematically, we expect the entanglement of spins in a region of size L_A (large compared to the lattice spacing) to be described by

$$S^{\text{local moments}}(l) = a_1 L_y L_A + a_2 L_y \log \min(L_A, L_B) + \cdots . \tag{6.3}$$

In the HFL phase, spins participate in the Fermi surface and we expect the area-law violating coefficient a_2 to be nonzero. The dependence on L_y and L_A may be understood by thinking of the 2D system on the torus as a collection of wires running in the x direction, one for each value of the conserved momentum k_y [35,36].

The mutual information between spins in A and spins in B conditioned on all itinerant electron degrees of freedom provides a subtraction scheme for subtracting out the volume law contribution in Eq. (6.3), thereby exposing the coefficient a_2. With the definitions in Fig. 9, for the case $l = L/2$ where A and B are each half of the spins, we have

$$I(A : B|C) = S_A + S_B - S_{AB} \sim 2a_2 L_y \log L_A . \tag{6.4}$$

Here we restrict ourselves to a mean-field treatment of the KLM where the local moments are represented by Abrikosov/slave fermions $\vec{S}_i = f^\dagger_{i\alpha} \vec{\sigma}_{\alpha\beta} f_{i\beta}$ [37,38]. When the Kondo coupling is sufficiently large, one obtains the HFL phase which is characterized by a mean field order parameter $V = \langle c^\dagger f \rangle$ representing the hybridization between c and f electrons.

Since the mean-field Hamiltonian is quadratic in fermion creation/annihilation operators, we can calculate the entanglement entropy of subsets of degrees of freedom using the correlation matrix technique [39]. Specifically, we consider a rectangular system of size $2L_y \times L_y$ and measure the mutual information between f electrons (or c electrons) in the left and right halves of the system. The results in the HFL phase are shown in Fig. 10. Entanglement entropy of f or c electrons alone follows a volume law. In contrast, their mutual information behaves as $I(A : B) \sim l \log l$, providing evidence that both f and c participate in the Fermi surface. We also studied the special case of $n_c = 1$, which corresponds to a Kondo insulator, and we find that the mutual information of both f and c saturates to an area law without any multiplicative logarithmic correction, as expected (Fig. 11, left).

When the Kondo screening is not operative, the mean field description of the system has $V = 0$. As mentioned above, a natural state with $V = 0$ is the FL* state. An alternative possibility that exists within mean field is an antiferromagnetic ordered state of local moments decoupled from the conduction electrons [40,41]. The right panel of Fig. 11 shows that, as expected, the mutual information of c fermions is Fermi-surface-like, while the f fermions are in a product state with no entanglement (an 'AFs' state [40,41] where 's' denotes small Fermi surface).

The mean field parameter V is not gauge invariant, and therefore it vanishes if the constraint $n_f = 1$ is implemented exactly. We propose that the conditional mutual information provides a gauge-invariant order parameter for the HFL phase and the FL* state. Although it is difficult to imagine measuring the mutual information experimentally for a macroscopic quantum system, it would be extremely interesting to implement our scheme within a Gutzwiller projected wave function where $n_f = 1$ is satisfied exactly on each site. We leave this for future work.

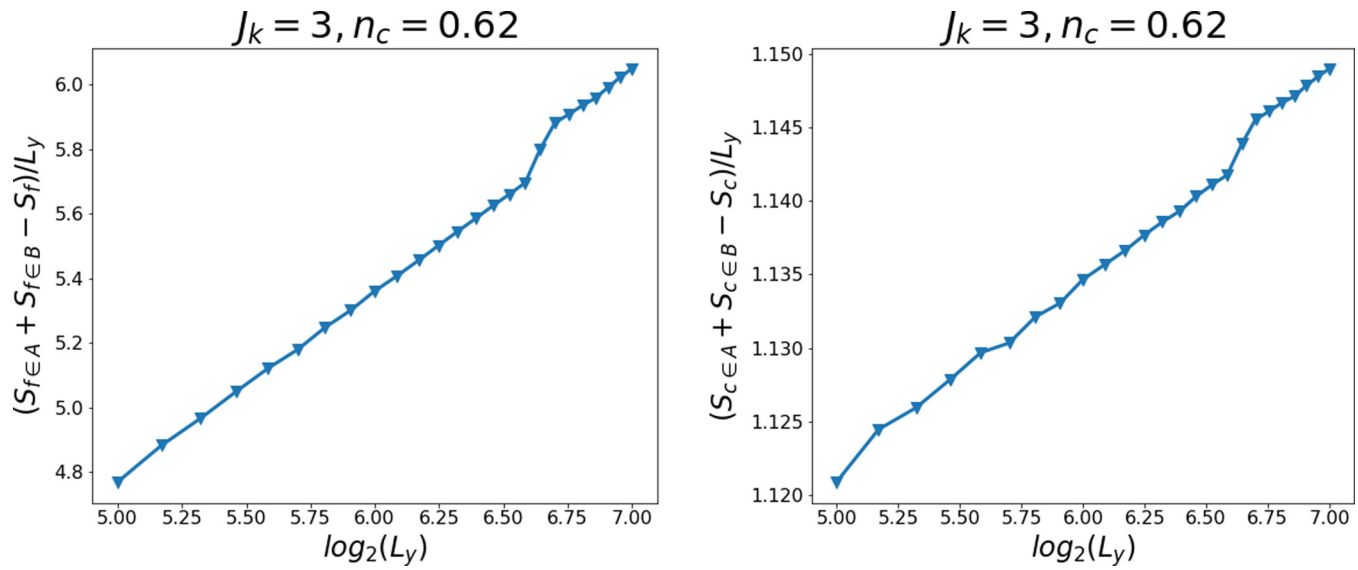

FIG. 10. Conditional mutual information calculated in the paramagnetic HFL phase, in mean field theory. The sample has dimensions $2L_y \times L_y$. It is bipartitioned into left and right $L_y \times L_y$ halves, A and B, as in Fig. 9; we vary the full system size L_y. Left: Conditional mutual information of f electrons as a function of system size, $I(f \in A : f \in B|c) = I(f \in A : f \in B)$. Right: Conditional mutual information of c electrons, $I(c \in A : c \in B|f) = I(c \in A : c \in B)$.

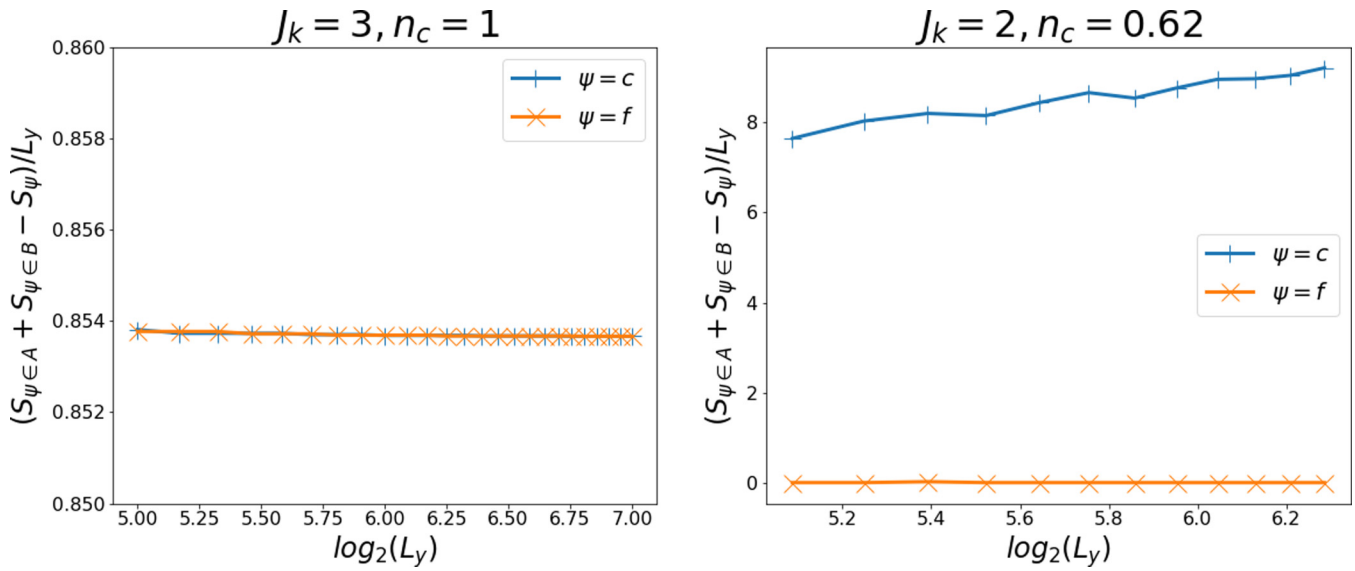

FIG. 11. In these plots we show conditional mutual information in different parts of the phase diagram, within mean field theory. Each plot shows both $S_{f\in A} + S_{f\in B} - S_f$ (crosses) and $S_{c\in A} + S_{c\in B} - S_c$ (vertical lines), in the geometry described in Fig. 9, as a function of overall system size L_y. Left: Conditional mutual information at a value of couplings in the HFL phase but at $n_c = 1$. Both curves exhibit a strict area law indicative of no Fermi surface. Right: Conditional mutual information calculated in the AFs phase. The conduction electrons show behavior indicative of a Fermi surface, while the local moment fermions do not.

VII. DISCUSSION

In this paper we generalized and employed the idea of quantum disentangled liquids (QDL) introduced in Ref. [8] in several different directions:

(1) We obtained a relation between the QDL quantity and conditional entropy, which provides an operator-agnostic definition of a QDL phase. In particular, we showed that in a finite energy eigenstate belonging to a QDL state, conditional entropy of light degrees of freedom is negative with a vanishingly small volume law coefficient, in contrast to an ergodic state, where it is positive, with an $O(1)$ volume law coefficient. In addition, we showed that the scaling of entanglement negativity can also sharply distinguish between a QDL state and an ergodic state.

(2) We argued that a QDL-based protocol can detect topological invariants in a gapless topological phases by studying a concrete model where charge degrees of freedom form a Luttinger liquid while the spin degrees of freedom are in an SPT state.

(3) We argued that a QDL-based protocol can be used to detect universal features of entanglement in Kondo lattice systems and can serve as an order parameter for a heavy Fermi liquid.

Further, we obtained several inequalities relating the QDL quantity to conditional information theoretic quantities.

Broadly speaking, our approach provides a way to characterize entanglement in multicomponent systems. It stands in contrast to more commonly used field-space entanglement [42–44], or particle-space entanglement [45,46], both of which lead to volume law entanglement even in the ground state of a local Hamiltonian due to nonlocal bipartitions of the Hilbert space. This makes it harder to separate universal contributions to entanglement entropy. In contrast, the measurement-based QDL quantity as well as conditional entropy follow an area law in the ground state (up to logarithmic corrections).

We derived several inequalities relating QDL quantity to operator-agnostic measures such as conditional entropy. These inequalities can be thought of as a manifestation of the monogamy of entanglement, which simply states that if party A is strongly entangled with party B, then it can't entangle strongly with another party C. For example, in the QDL phase, the light degrees of freedom with Hilbert space A are strongly entangled only with the heavy degrees of freedom in their immediate vicinity, which we denote as C. Therefore, measuring C disentangles A leading to an area-law scaling for the QDL quantity. Monogamy of entanglement implies that A would be unable to entangle with heavy degrees of freedom which are not in their immediate vicinity, and therefore, $S(AC) \approx S(C)$, leading to a small value for the conditional entropy $S(A|C)$.

Gapless topological phases are poorly understood in general. Examples in one dimension include Refs. [28,47,48] as well as the model in Eq. (4.1) from Ref. [22], the subject of our discussion in Sec. IV. As briefly discussed in Sec. VI, we expect that in a fractionalized Fermi liquid (the FL* phase) of Kondo lattice model, the conditional mutual information of local moments will satisfy an area law and also contain a subleading nonzero topological entanglement entropy (assuming that the local moments are in a gapped topological state). It will be interesting to extend this idea to gapless phases obtained via slave particle construction. Consider, for example, the Halperin-Lee-Read (HLR) state [49], which is a compressible quantum Hall state found in the half-filled Landau level. This phase can be understood in terms of a parton construction [50] $c = fb$ where c is the annihilation operator for the electron, the fermion f forms a Fermi liquid, and b forms an incompressible fractional quantum Hall state at $\nu = \frac{1}{2}$. The identification of diagnostics which reveal the topological order hidden in this gapless state

is a long-standing problem [51]. Might one be able to reveal it using the ideas described in this paper? For example, can one devise a procedure which projects out only the degrees of freedom corresponding to fermion f? A related question arises in the context of spin-3/2 spin chain, where it has been argued that despite the gapless spin degrees of freedom in the bulk, there still exist topological edge states [52]. Can one project out the effective spin-1/2 degrees of freedom to reveal the edge states corresponding to the effective spin-1 degrees of freedom?

A comment is in order about the use of measurement-based protocols for ground-state properties. One may have the impression that the projection onto the measurement outcome is a very violent operation. This makes it not obvious that the post-measurement wave function is still sensitive to subtle low-energy properties of the original state. However, a representation of the resulting amplitudes in terms of a path integral makes clear that the measurement projection only changes the *boundary conditions* on the path integral (at the Euclidean time slice where the wave function is evaluated) and therefore does not change its universal properties.

Finally, it will be interesting to consider implementing the measurement of QDL quantity in experiments to put bounds on conditional entropy using Eq. (1.1). Naively, when $|A| = O(1)$ and $|C| \gg 1$, one might think that QDL quantity can be measured without much difficulty by performing a projecting measurement on C followed by a state tomography on A. However, a major challenge with this approach is that state tomography requires an $O(|A|)$ destructive measurements on A, and the outcome of projective measurement on C prior to these destructive measurements should be *identical*. This is because the QDL quantity involves $S(\rho_A^c)$, the density matrix ρ_A^c on A for a fixed outcome c in C. This will be challenging when $|C| \gg 1$. Despite these difficulties, QDL quantity is easier to measure than the conditional entropy because the latter will require state tomography on C as well.

ACKNOWLEDGMENTS

We acknowledge useful discussions with and comments from Emily Davis, Tsung-Cheng Peter Lu, Alex Meill, Max Metlitski, Masaki Oshikawa, and Ashvin Vishwanath. This work was supported in part by funds provided by the US Department of Energy (D.O.E.) under cooperative research agreement DE-SC0009919. The work of J.M. is supported in part by the Simons Collaboration on Ultra-Quantum Matter. T.G. is supported by the National Science Foundation under Grant No. DMR-1752417 and as an Alfred P. Sloan Research Fellow.

APPENDIX A: DETAILS OF THE LOWER BOUND ON THE QDL DIAGNOSTIC

Here we give the full details of the proof that $S(A|C) \leqslant S_{\rm QDL}$.

$$S(A|C) \overset{(1,3)}{\leqslant} A - D(\mathcal{E}_C(\rho_{AC})||\mathcal{E}_C(u_A \otimes \rho_C)) \tag{A1}$$

$$= A - \mathrm{tr} \sum_c p_c \rho_A^c \otimes |c\rangle\langle c| \log \left(\sum_{c'} p_{c'} \rho_A^{c'} \otimes |c'\rangle\langle c'| \right) + \mathrm{tr} \sum_c p_c \rho_A^c \otimes |c\rangle\langle c| \log \left(\sum_{c'} p_{c'} u_A \otimes |c'\rangle\langle c'| \right) \tag{A2}$$

$$= A - \sum_c p_c \mathrm{tr}_A \rho_A^c \langle c| \left(\log \left(\sum_{c'} p_{c'} \rho_A^{c'} \otimes |c'\rangle\langle c'| \right) - \log \left(\sum_{c'} p_{c'} u_A \otimes |c'\rangle\langle c'| \right) \right) |c\rangle \tag{A3}$$

$$\equiv A + A_1 + A_2. \tag{A4}$$

To evaluate $A_{1,2}$ we must find the eigenbasis of the operators inside the log. The eigenvectors of $u_A \otimes \sum_{c'} p_{c'} |c'\rangle\langle c'|$ are $|a\rangle_A \otimes |c\rangle_C$ (where $\{|a\rangle\}$ is any basis for A) and the eigenvalues are $p_{c'} e^{-A}$. Therefore

$$A_2 = + \sum_c p_c \mathrm{tr}_A \rho_A^c \langle c| \left(\sum_{a,c'} (\log p_{c'} - A) |a\rangle\langle a|_A \otimes |c'\rangle\langle c'| \right) |c\rangle \tag{A5}$$

$$= \underbrace{\mathrm{tr}_A \rho_A^c}_{=1} \left(\sum_c p_c \log p_c - \sum_c p_c A \right) \tag{A6}$$

$$= -H(p) - A. \tag{A7}$$

The operator appearing in the log in A_1 is $\sigma \equiv \sum_{c'} p_{c'} \rho_A^{c'} \otimes |c'\rangle\langle c'|$. Let $|s_a^{(c)}\rangle$ be eigenvectors of ρ_A^c with eigenvalue $s_i^{(c)}$. Then

$$\sigma |s_a^{(c)}\rangle \otimes |c\rangle = \sum_{c'} p_{c'} \rho_A^{c'} |s_a^{(c)}\rangle \otimes |c'\rangle \underbrace{\langle c'|c\rangle}_{=\delta_{cc'}} = p_c s_a^{(c)} |s_a^{(c)}\rangle \otimes |c\rangle$$

so the eigenvectors of σ are

$$\left\{ |s_a^{(c)}\rangle \otimes |c\rangle \right\}, \quad a = 1 \ldots \dim \mathcal{H}_A, c = 1 \ldots \dim \mathcal{H}_C.$$

That is,

$$\sigma = \sum_{a,c} p_c s_a^{(c)} \left|s_a^{(c)}\right\rangle\!\left\langle s_a^{(c)}\right| \otimes |c\rangle\langle c|.$$

Therefore

$$A_1 = -\sum_c p_c \mathrm{tr}_A \rho_A^c \langle c| \log \sigma |c\rangle \tag{A8}$$

$$= -\sum_c p_c \mathrm{tr}_A \rho_A^c \langle c| \left(\sum_{a,c'} \left|s_a^{(c')}\right\rangle\!\left\langle s_a^{(c')}\right| \otimes |c'\rangle\langle c'| \log\left(p_{c'} s_a^{(c')}\right) \right) |c\rangle \tag{A9}$$

$$= -\sum_c p_c \mathrm{tr}_A \rho_A^c \underbrace{\sum_a \log\left(p_c s_a^{(c)}\right) \left|s_a^{(c)}\right\rangle\!\left\langle s_a^{(c)}\right|}_{=\log(p_c)+\log\rho_A^c} \tag{A10}$$

$$= -\sum_c p_c \mathrm{tr}_A \rho_A^c \log \rho_A^c - \sum_c p_c \log p_c \underbrace{\mathrm{tr}\rho_A^c}_{=1} \tag{A11}$$

$$= \sum_c p_c S\left(\rho_A^c\right) + H(p). \tag{A12}$$

Combining the three terms in (A4) we have

$$S(A|C) \leqslant A - H(p) - A + \sum_c p_c S\left(\rho_A^c\right) + H(p) \tag{A13}$$

$$= \sum_c p_c S\left(\rho_A^c\right) = \overline{S_{X_C}(A)}. \tag{A14}$$

APPENDIX B: CONDITIONAL MUTUAL INFORMATION IN THE HUBBARD MODEL

The CMI between regions A and B conditioned on C is

$$I(A:B|C) = S(AC) + S(BC) - S(ABC) - S(C).$$

In this expression, $S(A)$ refers to the entanglement entropy of spins *only* in region A, and $S(AB)$ is the total entanglement between spins and charge. In general, the CMI is a difference of conditional entropies

$$I(A:B|C) = S(AC) - S(C) - (S(ABC) - S(BC)) = S(A|C) - S(AB|C) \tag{B1}$$

and in this sense, our discussion here is not independent from the analysis of conditional entropy in the main text. In the case where ABC is the whole system [so ABC is a pure state and

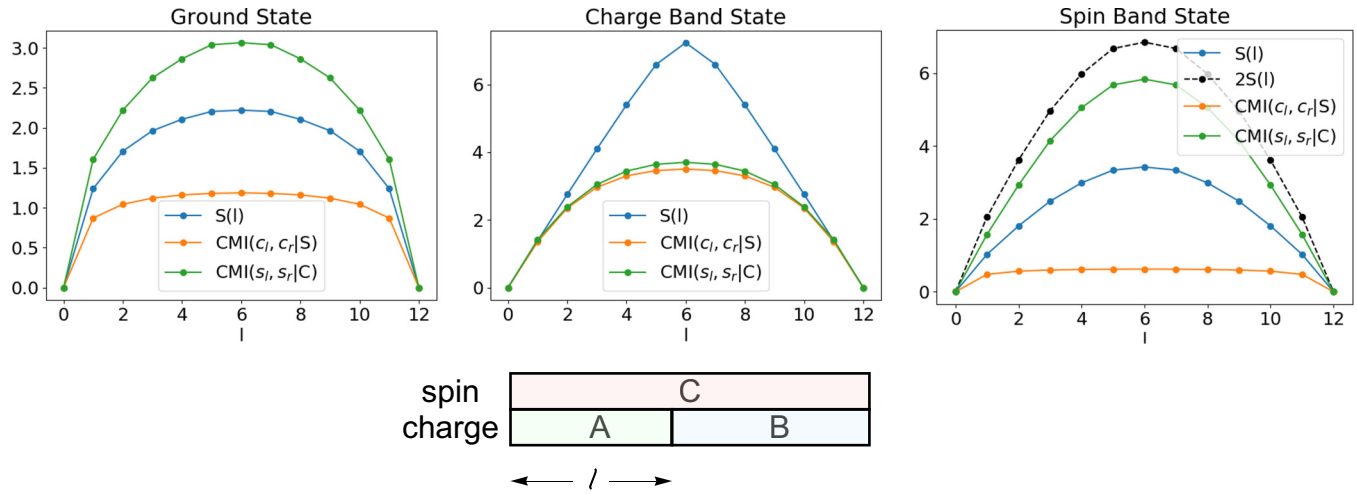

FIG. 12. Entanglement entropy and CMI measurements $I(A:B|C)$ on a one-dimensional Hubbard model as a function of the location of the bipartioning cut at couplings $U = 4$, $V = 3/4$. The chain is periodic and has $L = 12$ sites, the particle number is at half filling, and the magnetization is zero. Left: Ground state. Middle: A generic state in the charge band. Right: A state in the spin band. Bottom: $CMI(c|s)$ refers to CMI with the choice of subsystems indicated. $CMI(s|c)$ reverses the roles of spin and charge.

$S(AC) = S(B)$ etc.], the CMI reduces to $I(A : B|C) = I(A : B)$, the ordinary mutual information between A and B.

Expectations for the CMI can be found for ergodic and QDL states as in Sec. I B for various choices of A, B, C. Of the configurations we have explored, the one which distinguishes them most effectively is the arrangement shown in Fig. 3, where $A = C, B = D, A < B$. With this arrangement, in an ergodic state

$$I(A : B|C) = S(AC) - S(C) - S(AD) + S(D) \sim (A + C) - C - (D + A) + D = 2A. \quad \text{(B2)}$$

In a QDL state, we find

$$I(A : B|C) = S(AC) - S(C) - S(AD) + S(D) \sim C - C - (D + A) + D = A. \quad \text{(B3)}$$

The key effect is the missing A from $S(AC) \sim C$ in the QDL case, which happens since only the entanglement with C thermalizes A. This is precisely why conditional entropy distinguishes QDL from ergodic states, as described in Sec. I B.

So with this arrangement, both QDL and ergodic states give volume-law behavior of CMI but with distinct slopes. Taking advantage of this effect to compare different states would require a quantitative understanding of the coefficient of the volume law. This slope depends on $S(T)$, the entropy at the effective temperature of the state, which can be extracted from the von Neumann entropy of subsystems. However, since the effect is in any case not independent of the behavior of the conditional entropy, we choose not to pursue this direction further.

Results for CMI are presented in Fig. 12 for the particular arrangement of A, B, C indicated. We calculate CMIs $I(c_l : c_r|s)$, $I(s_l : s_r|c)$ as well as the bipartite von Neumann entropy S for the following three states obtained by exact diagonalization of 2.1: the ground state, a generic state taken from the middle of the spectrum, and a state belonging to the 'spin band,' i.e., a scar state.

There is indeed a visible difference in the behavior of the CMI between QDL states and ergodic states. However, a quantitative comparison with general expectations for the behavior of the CMI with the above arrangement of ABC is problematic for the following reason. Given a partition of a Hilbert space ABC where $\mathcal{H}_{AB}$ is the same size as $\mathcal{H}_C$, a finite energy density ergodic eigenstate should have $I(A : B) \sim \sqrt{L_A + L_B}$ after cancellation of the volume law terms [53,54].[5] This represents an area law as a function of L_A, while keeping $L_A + L_B$ fixed (as we do in Fig. 12). The calculation of Sec. I B shows that in a QDL state the CMI for this arrangement is also area law (the extensive terms cancel). So we attribute the different behavior seen in Fig. 12 to nonuniversal differences in the coefficient of the area law.

[5]The results of Refs. [53,54] follow from an ansatz [5,55] for the bipartition of an ergodic state in terms of a wave function which is a random matrix, which includes no information about the nature of the bipartition, such as locality. (Reference [53] matched these results to spatial bipartitions of a nonintegrable chain of hardcore bosons.) The conclusions depend only on the sizes of Hilbert spaces of subsystems with fixed charge. In particular, Ref. [54] generalizes the calculation to include several conserved quantities (the relevant conserved quantities here being spin, charge, and energy). As a result, we expect them to apply to our nonlocal bipartition of an eigenstate of a local Hamiltonian. The same conclusions about the leading terms would be obtained from a Haar-random pure state [16].

[1] J. M. Deutsch, Quantum statistical mechanics in a closed system, Phys. Rev. A **43**, 2046 (1991).

[2] M. Srednicki, Chaos and quantum thermalization, Phys. Rev. E **50**, 888 (1994).

[3] M. Rigol, V. Dunjko, and M. Olshanii, Thermalization and its mechanism for generic isolated quantum systems, Nature (London) **452**, 854 (2008).

[4] L. F. Santos, A. Polkovnikov, and M. Rigol, Weak and strong typicality in quantum systems, Phys. Rev. E **86**, 010102(R) (2012).

[5] J. M. Deutsch, Thermodynamic entropy of a many-body energy eigenstate, New J. Phys. **12**, 075021 (2010).

[6] L. D'Alessio, Y. Kafri, A. Polkovnikov, and M. Rigol, From quantum chaos and eigenstate thermalization to statistical mechanics and thermodynamics, Adv. Phys. **65**, 239 (2016).

[7] J. R. Garrison and T. Grover, Does a Single Eigenstate Encode the Full Hamiltonian? Phys. Rev. X **8**, 021026 (2018).

[8] T. Grover and M. P. Fisher, Quantum disentangled liquids, J. Stat. Mech.: Theory Exp. (2014) P10010.

[9] T. Veness, F. H. L. Essler, and M. P. A. Fisher, Quantum disentangled liquid in the half-filled Hubbard model, Phys. Rev. B **96**, 195153 (2017).

[10] T. Veness, F. H. Essler, and M. P. Fisher, Atypical energy eigenstates in the Hubbard chain and quantum disentangled liquids, Philos. Trans. R. Soc. London A **375**, 20160433 (2017).

[11] J. R. Garrison, R. V. Mishmash, and M. P. A. Fisher, Partial breakdown of quantum thermalization in a Hubbard-like model, Phys. Rev. B **95**, 054204 (2017).

[12] I. Marvian, Symmetry-protected topological entanglement, Phys. Rev. B **95**, 045111 (2017).

[13] M. Horodecki, J. Oppenheim, and A. Winter, Partial quantum information, Nature (London) **436**, 673 (2005).

[14] L. Henderson and V. Vedral, Classical, quantum and total correlations, J. Phys. A **34**, 6899 (2001).

[15] H. Ollivier and W. H. Zurek, Quantum Discord: A Measure of the Quantumness of Correlations, Phys. Rev. Lett. **88**, 017901 (2001).

[16] D. N. Page, Average Entropy of a Subsystem, Phys. Rev. Lett. **71**, 1291 (1993).

[17] J. Eisert and M. B. Plenio, A comparison of entanglement measures, J. Mod. Opt. **46**, 145 (1999).

[18] G. Vidal and R. F. Werner, Computable measure of entanglement, Phys. Rev. A **65**, 032314 (2002).

[19] N. E. Sherman, T. Devakul, M. B. Hastings, and R. R. P. Singh, Nonzero-temperature entanglement negativity of quantum spin models: Area law, linked cluster expansions, and sudden death, Phys. Rev. E **93**, 022128 (2016).

[20] T.-C. Lu and T. Grover (unpublished).

[21] U. T. Bhosale, S. Tomsovic, and A. Lakshminarayan, Entanglement between two subsystems, the Wigner semicircle and extreme-value statistics, Phys. Rev. A **85**, 062331 (2012).

[22] H.-C. Jiang, Z.-X. Li, A. Seidel, and D.-H. Lee, Symmetry protected topological Luttinger liquids and the phase transition between them, Sci. Bull. **63**, 753 (2018).

[23] F. D. M. Haldane, Continuum dynamics of the 1-D Heisenberg antiferromagnet: Identification with the O(3) nonlinear sigma model, Phys. Lett. A **93**, 464 (1983).

[24] I. Affleck, T. Kennedy, E. H. Lieb, and H. Tasaki, Rigorous Results on Valence-Bond Ground States in Antiferromagnets, Phys. Rev. Lett. **59**, 799 (1987).

[25] T. Kennedy and H. Tasaki, Hidden symmetry breaking and the Haldane phase in $S = 1$ quantum spin chains, Commun. Math. Phys. **147**, 431 (1992).

[26] F. Pollmann, A. M. Turner, E. Berg, and M. Oshikawa, Entanglement spectrum of a topological phase in one dimension, Phys. Rev. B **81**, 064439 (2010).

[27] T. Senthil, Symmetry-protected topological phases of quantum matter, Annu. Rev. Condens. Matter Phys. **6**, 299 (2015).

[28] R. Verresen, N. G. Jones, and F. Pollmann, Topology and Edge Modes in Quantum Critical Chains, Phys. Rev. Lett. **120**, 057001 (2018).

[29] R. Jozsa, D. Robb, and W. K. Wootters, Lower bound for accessible information in quantum mechanics, Phys. Rev. A **49**, 668 (1994).

[30] T. Senthil, S. Sachdev, and M. Vojta, Fractionalized Fermi Liquids, Phys. Rev. Lett. **90**, 216403 (2003).

[31] J. S. Hofmann, F. F. Assaad, and T. Grover, Fractionalized Fermi liquid in a frustrated Kondo lattice model, Phys. Rev. B **100**, 035118 (2019).

[32] F. Parisen Toldin, T. Sato, and F. F. Assaad, Mutual information in heavy-fermion systems, Phys. Rev. B **99**, 155158 (2019).

[33] D. Gioev and I. Klich, Entanglement Entropy of Fermions in Any Dimension and the Widom Conjecture, Phys. Rev. Lett. **96**, 100503 (2006).

[34] M. M. Wolf, Violation of the Entropic Area Law for Fermions, Phys. Rev. Lett. **96**, 010404 (2006).

[35] B. Swingle, Entanglement Entropy and the Fermi Surface, Phys. Rev. Lett. **105**, 050502 (2010).

[36] B. Swingle, Conformal field theory approach to Fermi liquids and other highly entangled states, Phys. Rev. B **86**, 035116 (2012).

[37] N. Read and D. Newns, A new functional integral formalism for the degenerate Anderson model, J. Phys. C: Solid State Phys. **16**, L1055 (1983).

[38] N. Read, D. M. Newns, and S. Doniach, Stability of the Kondo lattice in the large-N limit, Phys. Rev. B **30**, 3841 (1984).

[39] I. Peschel, Calculation of reduced density matrices from correlation functions, J. Phys. A: Math. Gen. **36**, L205 (2003).

[40] H. Watanabe and M. Ogata, Fermi-Surface Reconstruction without Breakdown of Kondo Screening at the Quantum Critical Point, Phys. Rev. Lett. **99**, 136401 (2007).

[41] M. Z. Asadzadeh, F. Becca, and M. Fabrizio, Variational Monte Carlo approach to the two-dimensional Kondo lattice model, Phys. Rev. B **87**, 205144 (2013).

[42] M. Taylor, Generalized entanglement entropy, J. High Energy Phys. 07 (2016) 040.

[43] M. R. Mohammadi Mozaffar and A. Mollabashi, On the Entanglement Between Interacting Scalar Field Theories, J. High Energy Phys. 03 (2016) 15.

[44] A. Mollabashi, N. Shiba, and T. Takayanagi, Entanglement between Two Interacting CFTs and Generalized Holographic Entanglement Entropy, J. High Energy Phys. 04 (2014) 185.

[45] O. S. Zozulya, M. Haque, K. Schoutens, and E. H. Rezayi, Bipartite entanglement entropy in fractional quantum Hall states, Phys. Rev. B **76**, 125310 (2007).

[46] C. M. Herdman, P.-N. Roy, R. G. Melko, and A. Del Maestro, Particle entanglement in continuum many-body systems via quantum Monte Carlo, Phys. Rev. B **89**, 140501(R) (2014).

[47] N. G. Jones and R. Verresen, Asymptotic correlations in gapped and critical topological phases of 1D quantum systems, J. Stat. Phys. **175**, 1164 (2019).

[48] R. Verresen, R. Thorngren, N. G. Jones, and F. Pollmann, Gapless topological phases and symmetry-enriched quantum criticality, arXiv:1905.06969.

[49] B. I. Halperin, P. A. Lee, and N. Read, Theory of the half-filled Landau level, Phys. Rev. B **47**, 7312 (1993).

[50] M. Barkeshli and J. McGreevy, Continuous transitions between composite Fermi liquid and Landau Fermi liquid: A route to fractionalized Mott insulators, Phys. Rev. B **86**, 075136 (2012).

[51] M. Barkeshli and J. McGreevy (unpublished).

[52] T.-K. Ng, Edge states in antiferromagnetic quantum spin chains, Phys. Rev. B **50**, 555 (1994).

[53] L. Vidmar and M. Rigol, Entanglement Entropy of Eigenstates of Quantum Chaotic Hamiltonians, Phys. Rev. Lett. **119**, 220603 (2017).

[54] C. Murthy and M. Srednicki, The structure of chaotic eigenstates and their entanglement entropy, Phys. Rev. E **100**, 022131 (2019).

[55] T.-C. Lu and T. Grover, Renyi entropy of chaotic eigenstates, Phys. Rev. E **99**, 032111 (2019).